Analogue experiments on compaction and shearing of wet granular media
Application to crystallizing magmas

Benoît Ildefonse, Katsuyoshi Michibayashi & Emmanuelle Cecchi
CNRS UMR 5568, Laboratoire de Tectonophysique, Université Montpellier II
benoit@dstu.univ-montp2.fr

1. Introduction

A remarkable characteristics of molten rocks is their radical changes in physical properties during crystallization or melting. This is the subject of an abundant literature, and some aspects of this physical evolution are still debated, like the values (melt volume fractions) of the thresholds that corresponds to changes in the magma rheology and/or deformation mechanisms. The major change corresponds to the full connection of the solid, crystalline phase, generally referred to as "critical melt fraction" (CMF). The rigid, solid backbone being locked, the deformation of the magmatic mush may continue only by deforming the crystals; true suspension flow is not possible anymore. Whatever the involved deformation mechanism, such a change will be recorded by the rock microstructures. In spite of the relatively simple definition of this threshold, its value remains poorly constrained (proposed values range from 20 to 70% melt. Fig. 1), and the concept itself of the MCF is still debated (e.g. Rushmer, 1996; Bagdassarov and Dorfmann, 1998).

We present preliminary results of analogue experiments on compaction and shearing of wet granular media, designed to re-examine this threshold and its variations with i) the particle size and shape, and ii) the deformation regime.

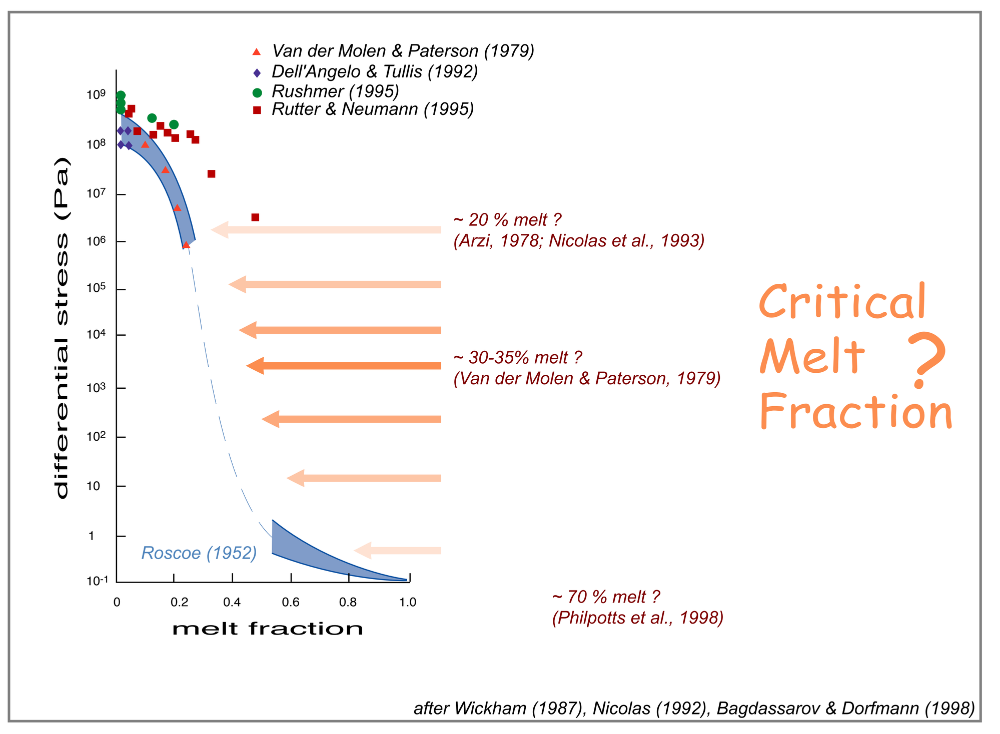

Fig. 1 - Strength of partially molten rocks. Proposed values of the critical melt fraction range from 20 to 70% volume melt. Recent experimental data do not match the classical experimental curve of Van der Molen & Paterson (1979).

2. Experimental device

The apparatus was specifically designed for these experiments. It is very simple : suspensions of rigid particles (PVC cylinders, glass beads, ...) are placed in a glass tube (diameter 15 cm), and compressed and/or sheared by a piston (Fig. 2a and b). Compression is induced by the weight of the piston, rotation is induced by a small motor (Fig. 2b and c). As the piston goes down, the fluid is progressively expelled at the edges of the model. The maximum compaction (particle locking threshold) is attained when the piston cannot go down anymore. The displacement and the rotation of the piston are continuously recorded by transducers (Fig. 2b and c), and the experimental set-up also allows one to capture series of video images of the model during the experiments.

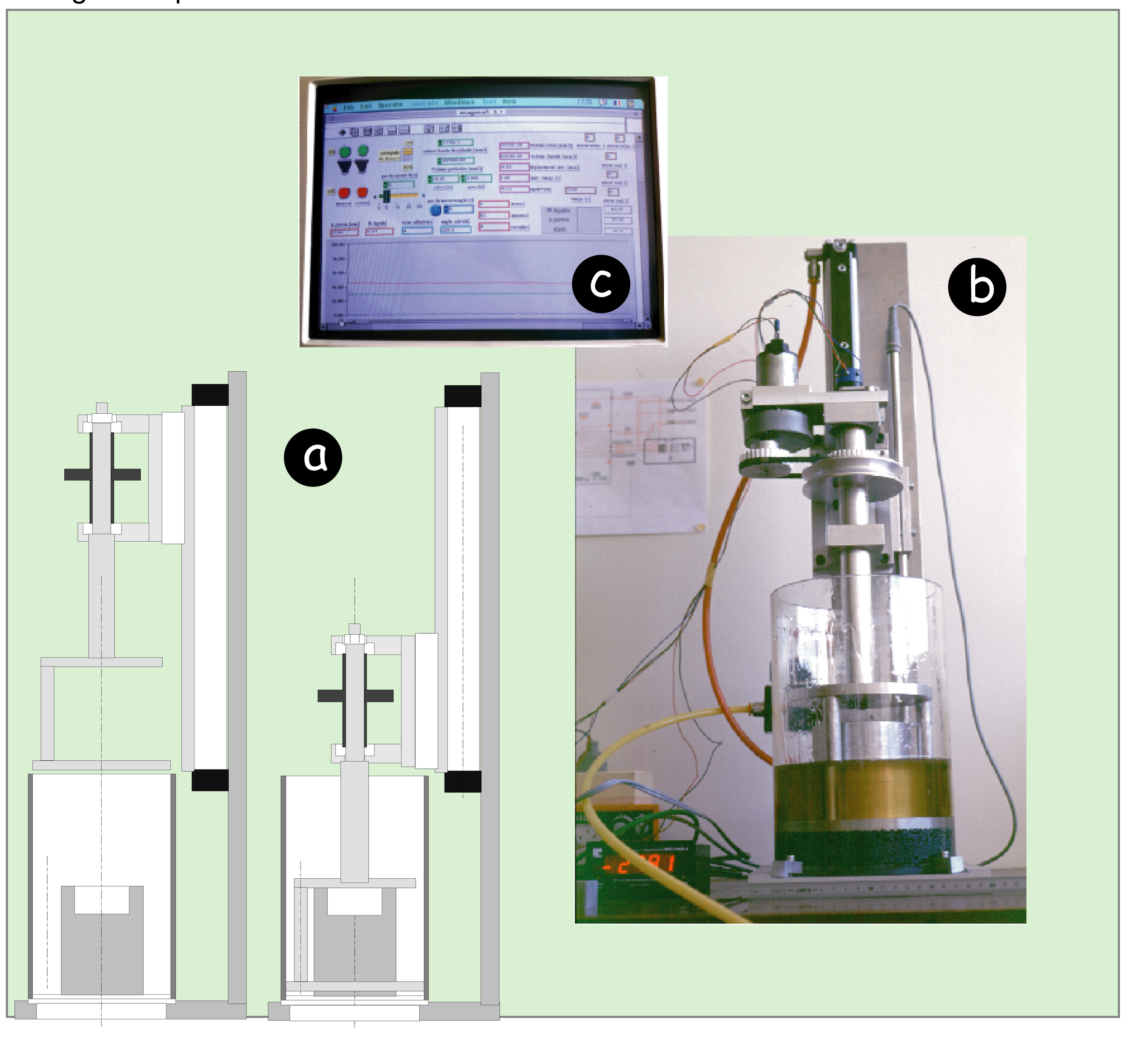

Fig. 2 - Experimental device

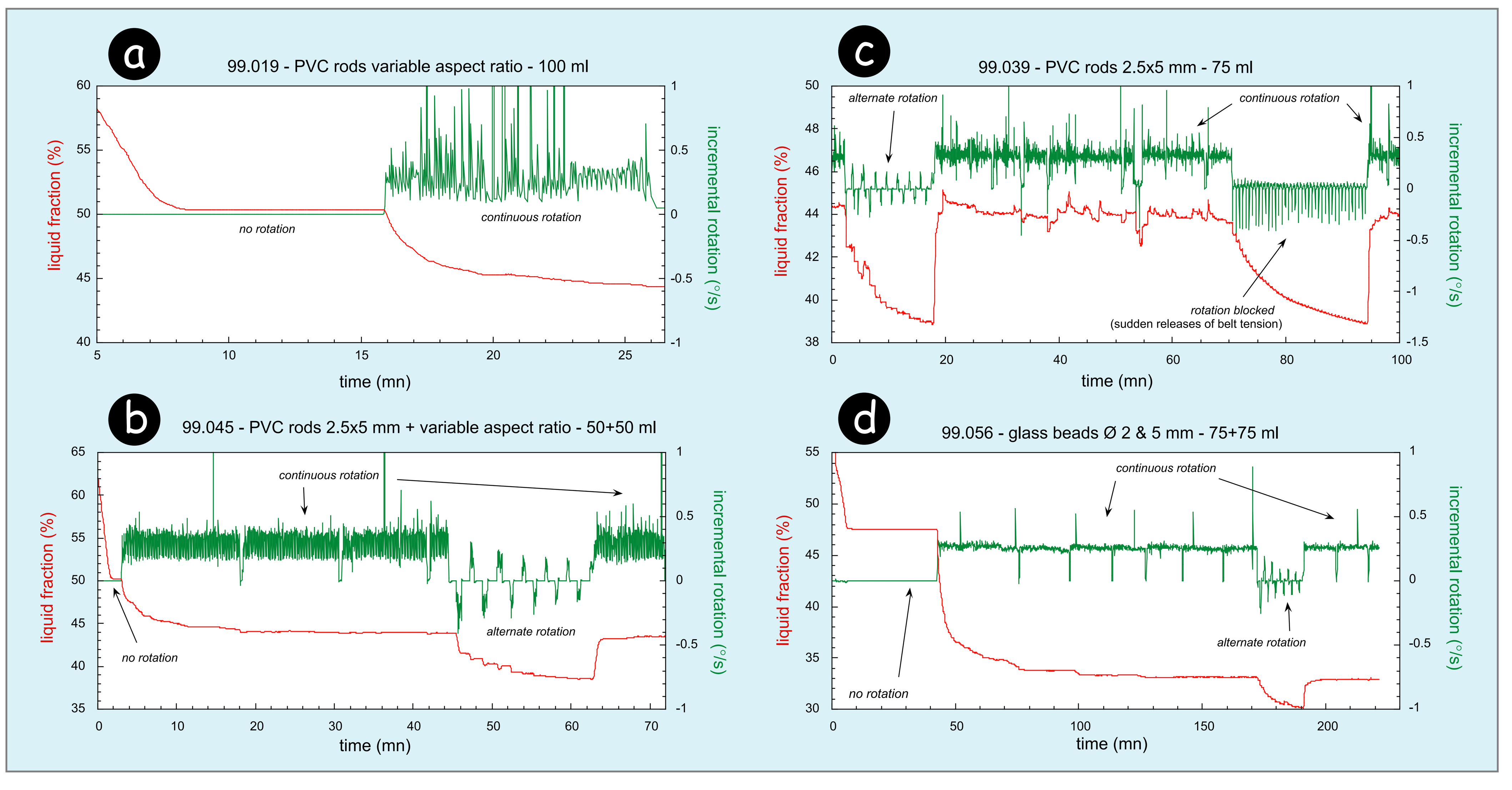

Fig. 3 - Some examples of experimental curves

3. Summary of experimental results

Three distinct thresholds are attained depending on the deformation regime (Figs 3 &4).

1 • The piston does not rotate: The liquid fraction remains > 45 % in all cases. It varies a lot (Fig. 4a) as it depends strongly on the heterogeneous distribution of the particle population at the beginning of the experiments.

2 • Continuous, one-sense shearing is applied: In all experiments, this results in a significant decrease of the liquid fraction (Fig. 3a, b & d); the threshold decreases to a minimum of 38% (Fig. 4b) for experiments with population of particles of similar sizes, and to a minimum of 32 % for experiments with a bimodal size distribution (Fig. 3d and 4b).

3 • Maximum compaction is achieved by applying alternate rotation increments to the piston (Fig. 3b, c & d). The threshold decreases to a minimum of 35% (Fig. 4c) for experiments with population of particles of similar sizes, and to a minimum of 30 % for experiments with a bimodal size distribution (Fig. 3d and 4c). The same results is obtained when the piston rotation is blocked (particle locking) : the motor transmission belt periodically jumps to the next gear tooth, resulting in a sudden release of the stress and a small, rapid reverse rotation increment.

Shape preferred orientations are calculated from projected images of experiments (Fig. 5c & d). The fabric ellipse is calculated using the 2D orientation tensor defined by Harvey & Laxton (1980). The developed fabric is significantly stronger with long rods (average n=3.37) than with short ones (n=2) (Fig. 5a). In both cases, the fabric orientation is similar; it always remains oblique to the shear plane, with the same relative orientation (ranges from 0 to 15°. Fig. 5b).

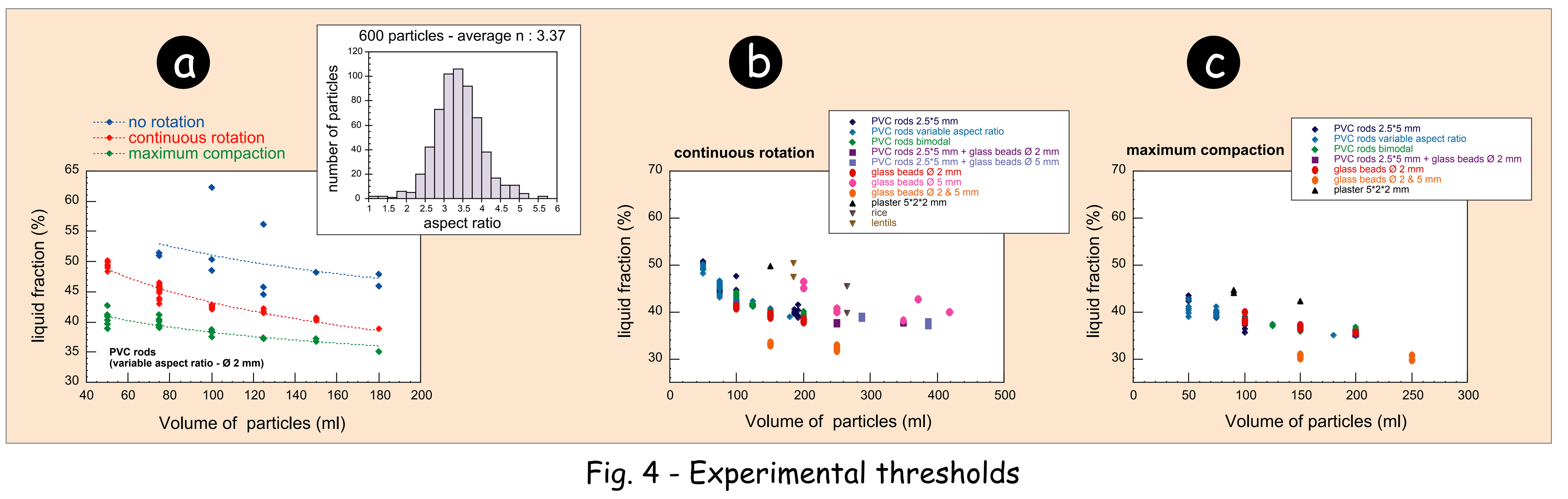

Fig. 4 - Experimental thresholds

4. (some elements for a) Discussion and Conclusion

• Continuous shearing is not the best way to reduce the locking threshold in a concentrated suspension. This is explained by the dilatance that occurs in any granular medium when sheared (e.g. Evesque & Lanos, 1997).

• The lower possible thresholds are achieved when conducting alternate rotation of the piston. This process is similar to shaking, which classically improves compaction of granular media. although it is difficult to imagine this type of oscillating regime of deformation in nature, we suggest that earthquakes may have the same effect on the CMF of a magmatic mush in a seismogenic environment (i.e. magma chambers at oceanic spreading ridges).

• There is a significance decrease of the observed threshold when increasing the volume of particles (Fig. 4). This is clearly a bias inherent to our experimental device. However, we cannot use very thick models because of the strong vertical shear gradient (shearing is applied only at the upper boundary).

• There is only a minor effect, if any, of the shape of the particles (Fig. 4) on the threshold. Beads and rods give similar results. However, these two shapes are more efficient to reduce the threshold than more complicated ones (plaster rectangular prisms, rice, lentils. Fig. 4b & c). Surprisingly, the better fabric in the experiments with longer rods (Fig. 5) seems to have no effect on the threshold value.

• The most important effect on reducing the locking threshold is the variation in grain size (experiments with two sizes of glass beads, Ø 2 & 5 mm. Fig. 3d, 4b & c). This effect now needs to be further investigated with a new series of experiments.

In most of our experiments (nearly mono-size particle populations), the CMF was not lower than 35%. In any case, the minimum possible value was 30% (maximum compaction, bimodal particle size population).

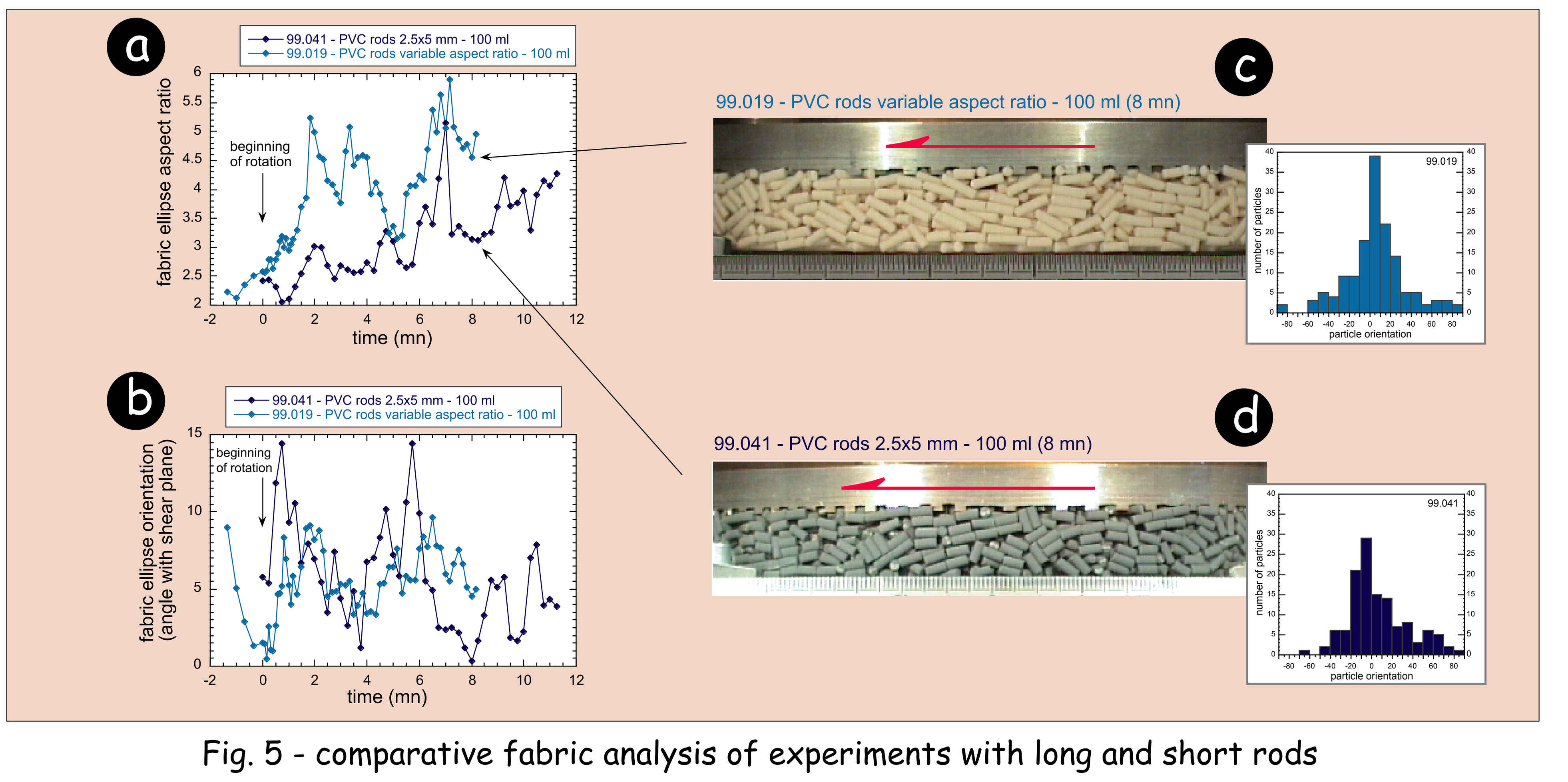

Fig. 5 - comparative fabric analysis of experiments with long and short rods

References

• Arzi, A.A., 1978. Critical phenomena in the rheology of partially melted rocks. Tectonophysics, 44: 173-184.
• Bagdassarov, N. and Dorfman, A., 1998. Granite rheology: magma flow and melt migration. J. Geol. Soc., 155: 863-872.
• Evesque, P. and Lanos, C., 1997. La mécanique du sable mouillé. In: "Des grands écoulements naturels à la dynamique du tas de sable. Introduction aux suspensions en géologie et en physique" (B. Ildefonse, C. Allain & P. Coussot, eds). Cemagref Editions, pp. 231-252.
• Harvey, P.K. and Laxton, R.R., 1980. The estimation of finite strain from the orientation distribution of passively deformed linear markers ; eigenvalue relationships. Tectonophysics, 70: 285-307.
• Nicolas, A., 1992. Kinematics in magmatic rocks with special reference to gabbros. J. Petrology, 33: 891-915.
• Nicolas, A., Freydier, C., Godard, M. and Vauchez, A., 1993. Magma chambers at oceanic ridges : how large ? Geology, 21: 53-56.
• Philpotts, A.R., Shi, J. and Brustman, C., 1998. Role of plagioclase crystal chains in the differentiation of partly crystallized basaltic magma. Nature, 395: 343-346.
• Rushmer, T., 1996. Melt segregation in the lower crust: How have experiments helped us? Transactions of the Royal Society of Edinburgh - Earth Sciences, 87: 73-83.
• Van der Molen, I. and Paterson, M.S., 1979. Experimental deformation of partially-melted granite. Contr. Miner. Petrol., 70: 299-318.
• Wickham, S.M., 1987. The segregation and emplacement of granitic magmas. J. Geol. Soc. London, 144: 281-297.